The Variability of Seasonality

S. PEZZULLI, D. B. STEPHENSON, AND A. HANNACHI

Department of Meteorology, University of Reading, Reading, United Kingdom

(Manuscript received 15 August 2003, in final form 1 July 2004)

ABSTRACT

Seasons are the complex nonlinear response of the physical climate system to regular annual solar forcing. There is no a priori reason why they should remain fixed/invariant from year to year, as is often assumed in climate studies when extracting the seasonal component. The widely used econometric variant of Census Method II Seasonal Adjustment Program (X-11), which allows for year-to-year variations in seasonal shape, is shown here to have some advantages for diagnosing climate variability. The X-11 procedure is applied to the monthly mean Niño-3.4 sea surface temperature (SST) index and global gridded NCEP–NCAR reanalyses of 2-m surface air temperature. The resulting seasonal component shows statistically significant interannual variations over many parts of the globe. By taking these variations in seasonality into account, it is shown that one can define less ambiguous ENSO indices. Furthermore, using the X-11 seasonal adjustment approach, it is shown that the three cold ENSO episodes after 1998 are due to an increase in amplitude of seasonality rather than being three distinct La Niña events. Globally, variations in the seasonal component represent a substantial fraction of the year-to-year variability in monthly mean temperatures. In addition, strong teleconnections can be discerned between the magnitude of seasonal variations across the globe. It might be possible to exploit such relationships to improve the skill of seasonal climate forecasts.

1. Introduction

The annual march of the Earth around the Sun provides a periodic solar forcing that acts as a strong pacemaker for the general circulation of the terrestrial climate. The resulting seasons that we observe are the complex nonlinear response of the atmosphere, land, and oceans and represent one of the most important variabilities of the climate system. Unlike the external solar forcing, which varies very little from year to year, there is no guarantee that climatic seasons have to be the same each year. This has been apparent to many generations of farmers, who have been aware of the vagaries in the sowing times, or satiōns in Latin, from which the word *season* originates.

The variability of seasonality is not something new in climate research. For example, Cook et al. (2000) pointed out that El Niño–Southern Oscillation (ENSO) has exhibited large changes in the amplitude/phase of the annual cycle as well as in the frequency/intensity of warm/cold events in the past century as shown from instrumental observation record. Thompson (1995) and Thomson (1995) addressed the issue of varying seasonality using complex demodulation. Thompson (1995) found coherent phase/amplitude changes in the annual cycle of temperature records at six different stations across Europe. Thomson (1995) suggested that changes in the annual cycles may be caused by changes in the Sun's luminosity and greenhouse gas, that is, atmospheric CO_2 concentration. He found that doubling CO_2 concentration can decrease the amplitude of the annual cycle in global temperature. Van Loon et al. (1993) analyzed seasonality in monthly mean of pressure and wind in the Southern Hemisphere. They showed that the annual cycle has undergone zonal asymmetric changes.

The climate response to the annual cycle in solar forcing is complex. Note that one should not refer to the *annual cycle* as the *seasonal cycle* since the period is one year not one season (cf. diurnal cycle; K. E. Trenberth 1996, personal communication). Due to nonlinearities in the climate system, the climate response to the annual cycle in solar forcing can be surprisingly abrupt (e.g., the rapid onset of the Asian monsoon). The periodic solar forcing is rectified by nonlinearities to give higher-frequency harmonics such as the semiannual oscillation, which is particularly dominant in the western equatorial Pacific (van Loon and Jenne 1970; Meyers 1982). In addition, endogenous (internal) modes of variability such as ENSO can lead to subharmonic variations such as the tropospheric quasi-biennial (2 yr) and quasi-quadrennial (4 yr) oscillations (e.g., Rasmusson and Carpenter 1982; Rasmusson et al. 1990; Tziperman et al. 1994; Jiang et al. 1995; Jin et al.

Corresponding author address: Dr. S. Pezzulli, Department of Meteorology, University of Reading, Earley Gate, P.O. Box 243, Reading RG6 6BB, United Kingdom.
E-mail: S.Pezzulli@reading.ac.uk

1994, 1996; and references therein). Such harmonics whose periods are rational multiples of the annual harmonic give rise to synchronized interannual anomalies, occurring at preferred times of the year. *Phase locking* of interannual anomalies to the annual cycle is evident in many modes of climate variability: the monsoons, ENSO, the North Atlantic Oscillation, etc. The phase locking of subharmonics with the annual cycle is responsible for variations in the Peru Current at Christmastime that led to ENSO warm events being named El Niño by Peruvian fishermen (Philander 1990). Studies have shown that interannual variations such as ENSO can modulate the annual cycle of tropical Pacific temperatures (Chang et al. 1995; Gu and Philander 1995; Gu et al. 1997; Yu and McPhaden 1999; and references therein). The existence of nonlinearities and phase locking imply that the seasonal and interannual variability can mutually interact, and as such, the problem of separating out the different signals becomes intricate and should be performed with care.

The traditional approach in most climate studies is to treat the annual cycle as a fixed mean effect that does not vary from year to year. For monthly data, for example, the mean annual cycle is estimated by averaging the climate variable for each calendar month separately over all the available years. The mean annual cycle is then subtracted from the original data to give what is referred to as an *anomaly* from the mean annual cycle. These anomalies are widely used in climate studies to characterize variability. This approach is based on the (unjustifiable) assumption that the annual cycle is a constant from year to year. However, interannual variations in the annual cycle can be seen in many climate time series (see, e.g., Thompson 1999; Bograd et al. 2002; Whitfield et al. 2002; and references therein) and deserve more careful attention. The traditional approach can incorrectly mix up these fluctuations of the annual cycle with longer-term variations in the mean.

In this study, we propose and demonstrate a more flexible alternative approach that can allow for varying seasonality. Section 2 reviews the traditional approach in more depth and introduces the econometric variant of Census Method II Seasonal Adjustment Program (X-11) that is frequently used in economics to model seasonality. Results obtained with this approach for ENSO indices and global gridded monthly mean surface temperature data are presented in section 3. Conclusions and suggestions for future extensions are given in section 4.

2. Methods

In general, observed and model-simulated climate data have equally spaced sample time intervals and thereby consist of regular time series of the form X_t, $(t = 1, 2, \ldots, N)$. The period of 1 yr is defined to be an integer number (p) of sample times. For the monthly mean data studied here, the sample time is 1 month and hence there are $p = 12$ sample times in 1 yr. The results are completely general and are applicable for other sampling times such as daily or seasonal.

a. The traditional approach

The annual cycle for any particular year y, is fully described by the p-dimensional vector, $\mathbf{x}_y$, containing the p successive time series values for that year. The complete time series for n yr can be therefore considered as a yearly sequence of p-dimensional vectors and can be usefully represented by the $(p \times n)$ rectangular *data matrix* $\mathbf{X}$:

$$\mathbf{X} = (\mathbf{x}_1, \mathbf{x}_2, \ldots, \mathbf{x}_n) = \begin{pmatrix} x_{11} & x_{12} & \cdots & x_{1n} \\ x_{21} & x_{22} & \cdots & x_{2n} \\ \vdots & \vdots & & \vdots \\ x_{p1} & x_{p2} & \cdots & x_{pn} \end{pmatrix},$$

where $n = N/p$ is the total number of years and the element x_{my} is the value at sample time (e.g., month) m of year y.

The data matrix $\mathbf{X}$ completely summarizes the time series and can be represented as a numeric table. It also can be mapped using colors and/or contour lines to give a visual representation (as shown later in Fig. 3).

The ensemble of n annual vectors $\mathbf{x}_y$ describe a cloud of n points in p-dimensional seasonal-state space. The mean annual cycle $\mathbf{c}$ is the center of mass of the cloud, obtained by averaging over the columns of the data matrix. The seasonal time series, C_t, is the periodic extension of $\mathbf{c}$ replicated n times to produce a time series of length N.

Fluctuations about the mean annual cycle can be obtained by considering the *anomalies* $\mathbf{x}'_y = \mathbf{x}_y - \mathbf{c}$. The anomalies can also be represented either as a matrix or as a time series $X'_t = X_t - C_t$. The matrix elements will be denoted by x'_{my}.

The annual mean of the anomalies, a_y, is a simple way to filter out annual and subannual variations and retain the interannual variations. It is equivalent to assuming that each year has a specific constant effect on the series, and the interannual variations are modeled by mean-level *jumps* between years. In other words, the corresponding series of the interannual variations, A_t, replicates p times a_1, for all t in the first year, then becomes a_2 in the second year and so on, that is, a piecewise-constant and discontinuous evolution.

The centered annual cycle $\tilde{\mathbf{c}}$ is obtained by subtracting out the long-term mean $\mu = \bar{x}$ of the original series from the annual cycle. Hence the generic element of the centered annual cycle is

$$\tilde{c}_m = c_m - \mu,$$

representing the net seasonal response for season m. Denoting by $\tilde{C}_t$ the periodic extension of $\tilde{\mathbf{c}}$, we obtain the additive decomposition

$$X_t = \mu + \tilde{C}_t + A_t + R_t, \quad (1)$$

where by construction the seasonal effect $\tilde{C}_t$ is periodic while the interannual effect A_t is a piecewise constant. Both seasonal and annual effects are net (or centered) components, that is, have zero means. The value R_t represents irregular residual variations such as subannual fluctuations.

Annual and seasonal means calculated in this traditional way are the best least squares fit for the two-way analysis of variance (ANOVA) model (see appendix A).

For obtaining a continuous trend component, a standard approach for ENSO studies is the 5-month running mean of the anomalies

$$A_t^* = \mathrm{MA}_5(X_t') = \frac{1}{5}\sum_{\tau=t-2}^{t+2} X_\tau',$$

while the subannual terms are given by the residual series $R_t^* = X_t' - A_t^*$. This yields the decomposition

$$X_t = \mu + \tilde{C}_t + A_t^* + R_t^*. \quad (2)$$

Note that additivity is assumed in both the traditional decompositions (1) and (2); that is, the constant level, interannual, seasonal, and irregular terms sum up to the original datum. It is good practice to question this additivity assumption, but usually this is not done.

b. The X-11 seasonal adjustment procedure

Numerous bandpass filtering methods have been developed in order to remove the seasonal component from (*seasonally adjust*) economic indices such as commodity prices and unemployment rates (Franses 1996). In this study, we adopt a simple and flexible method known as the X-11, which is currently used to produce official statistics and various analyses in many national institutions and central banks around the world. Introduced in 1965 by the U.S. Census Bureau, it was the product of over a decade of development beginning with Method I in 1954, followed by twelve variants (X-0, X-1, etc.) of Method II, culminating in X-11 (Shiskin et al. 1967; Shiskin 1978). Further contributions were added to the basic version of the seventies, including regression and Autoregressive Integrated Moving Average (ARIMA) modeling (for a detailed account see Findley et al. 1998). Here, we will define and use a simple version of the basic procedure.

The X-11 procedure generates the decomposition

$$X_t = T_t + S_t + I_t, \quad (3)$$

where T_t is the trend component, corresponding to the traditional uncentered trend $\mu + A_t$ (or $\mu + A_t^*$ when the five-term running mean is used), S_t is the net seasonal term corresponding to the traditional centered seasonal term $\tilde{C}_t$, and the residual I_t is the irregular variation corresponding to the traditional subannual term R_t (or R_t^*).

We have stated that the traditional approach, and in particular the additive decomposition (1), can be seen as the least squares solution of the two-way ANOVA model. The X-11 procedure, on the other hand, may be seen as a straightforward extension of the two-way approach, in order to provide a continuous interannual trend, T_t, and a *quasi-periodic* seasonal term S_t (see appendix A). The main reason for allowing a variable annual cycle is that interannual nonseasonal fluctuations in economic growth cycles are known to modulate seasonal fluctuations. For example, New Year shopping sales can be adversely affected by recessions (Franses 1996).

The X-11 method can be defined by a three-step filtering algorithm. For monthly data it proceeds as follows (with trend and seasonal filters as defined in appendix B):

1) Initial trend and seasonal estimates
   (a) Estimate the T_t component by the annual-centered running mean: $T_t = \mathrm{MA}_{2\times12}(X_t)$.
   (b) The trend-adjusted series $Z_t = X_t - T_t$ represents seasonality and shorter-term noise only. Thus a seasonal running mean $\mathrm{SMA}_{2\times2}$ of the trend-adjusted series, Z_t, can be applied without confusing trend and seasonal signals. The resulting (seasonal) series is finally adjusted by subtracting its annual-centered running mean $\mathrm{MA}_{2\times12}$, which will approximately produce a zero mean seasonality.
2) Revised trend and seasonal estimates
   (a) Repeat step 1a on the seasonally adjusted series $Y_t = X_t - S_t$ to obtain an improved estimate of $T_t = \mathrm{MA}_{2\times12}(Y_t)$. Note that trend filters work better on seasonally adjusted series than on original data.
   (b) Repeat step 1b on the revised trend-adjusted series $Z_t = X_t - T_t$.
3) Final trend and irregular estimates
   Repeat step 2a on the revised seasonally adjusted data $Y_t = X_t - S_t$ and finally compute the residual series $I_t = X_t - T_t - S_t$. The seasonal series of the previous step is left unchanged.

The algorithm consists of an alternate trend estimation on seasonally adjusted series and seasonal estimation on the trend-adjusted one. Usually, for trend estimation in steps 2a and 3, the centered annual running mean is replaced by the Henderson trend filter (Henderson 1916), which produces a smooth local cubic polynomial trend. The filter is defined by the number h of weights. In this paper, we used $h = 23$ (see section 2d).

Main features of the X-11 decomposition (3) are that the trend does not contain the annual cycle or its higher

harmonics, any consecutive 12-month mean of the seasonal term is approximately zero, and the seasonal term is defined locally in time.

c. Spectral filtering properties of X-11 and traditional procedures

The combined action of the preceding three steps can be more simply described as the effect of filtering the data with a low bandpass filter T_t, a seasonal filter S_t, and a high-pass filter I_t. The properties of these symmetric filters can be studied by considering their effect on the component of frequency ω of the input series. The spectral densities of input and filtered output series, say $f_1(\omega)$ and $f_2(\omega)$, are related by

$$f_2(\omega) = |g(\omega)|^2 f_1(\omega), \tag{4}$$

where g is the frequency response function

$$g(\omega) = \sum_{j=-m}^{m} \alpha_j e^{-i\omega j},$$

and $\{\alpha_j; j = -m, -m + 1, \ldots, m\}$ are the filter weights.

The frequency response modulus $|g(\omega)|$ is called the gain and the squared gain

$$G(\omega) = |g(\omega)|^2$$

is known as the *power transfer function* of the filter (Bloomfield 1976). From Eq. (4) the power transfer function $G(\omega)$ represents the extent to which the contribution of the component of frequency ω to the total variance of the series is modified by the action of the filter.

Figure 1 shows the power transfer function for the X-11 filters (solid lines) compared to the power transfer function of the components obtained using the traditional fixed season approach on a 50-yr-long monthly series (dashed lines). The annual cycle has (nonangular) frequency $f = 12\omega/(2\pi) = 1$, and has higher (subannual) harmonics $f = 2, 3, 4, 5$, and 6, corresponding to waves of periods 6, 4, 3, 12/5, and 2 months, respectively.

Whereas the spectral transfer properties of X-11 do not depend on the length of the time series, the transfer properties of the traditional approach have the disadvantage that they do depend on the length of the time series. This in practice produces a distortion effect (see Fuenzalida and Rosenblüth 1986), which is evident in the power transfer function. The sample size used here is the same as that of the data analyzed later. For shorter time series, the transfer functions of the traditional approach become more spread out and the method separates out less well seasonal variations from interannual variations (not shown).

The solid line in Fig. 1a shows that the power transfer function of the X-11 trend filter acts as a good bandpass filter for $f < 1$ (interannual variations). In contrast, the transfer function for the traditional 5-month running mean anomaly transfer function (dashed line in Fig. 1a) allows substantial amounts of subannual power to leak through into the higher-frequency subannual range.

The seasonal X-11 filter lets power pass through at the annual frequency and harmonics and neighboring frequencies (Fig. 1b). Leakage around the harmonics is essential for obtaining a variable seasonal component since an impulsive power transfer function (e.g., the traditional seasonal component—dashed line in Fig. 1b) gives a perfectly periodic seasonality. The irregular component power transfer functions shown in Fig. 1c indicate that the X-11 approach has a more smooth and uniform response for all subannual nonharmonic components, whereas the traditional approach has irregular behavior near harmonics and has a maximum response for frequencies between 3 and 4 (i.e., periods between 3 and 4 months).

The traditional approach exhibits complicated filter behavior close to the annual frequency, both in trend and irregular terms. Finally, Fig. 1 indicates that when many quasi-annual frequencies are important modes of variability, so that the annual cycle is subjected to interannual variations, these are almost completely added to the trend component, under the traditional approach, but they are correctly included in the seasonal component by X-11.

The different spectral behavior is related to differences in the autocorrelation of the series. The X-11 irregular component exhibits negative autocorrelation at 12 months, whereas the traditional irregular component has negative autocorrelations at shorter lags of 1 and 2 months. Such negative autocorrelations are the consequence of using moving-average filters in both approaches.

One might be tempted to use Fourier filtering instead of the X-11 procedure. However, an important difference between X-11 and Fourier filtering is that X-11 is local in time whereas Fourier filtering is nonlocal in time and uses data from all the time series. The local property of X-11 is an advantage when dealing with time series where seasonality can be severely disrupted during specific events (e.g., strong El Nino events such as 1982/83). X-11 provides a robust local estimate of the seasonality in a particular year influenced only by recently preceding and proceeding years.

d. Calibrating X-11

As mentioned at the end of section 2b, the X-11 procedure can be defined in different ways depending on alternative filters. Other common variants include using Henderson trend filters with $h = 13$ and $h = 17$, and the seasonal running means $\mathrm{SMA}_{3\times3}$ and $\mathrm{SMA}_{3\times5}$.

For the Henderson filter, lengths shorter than $h = 23$ would produce an undesirable subannual peak in the transfer function between one and two cycles per year.

For the choice of the seasonal filter, note that

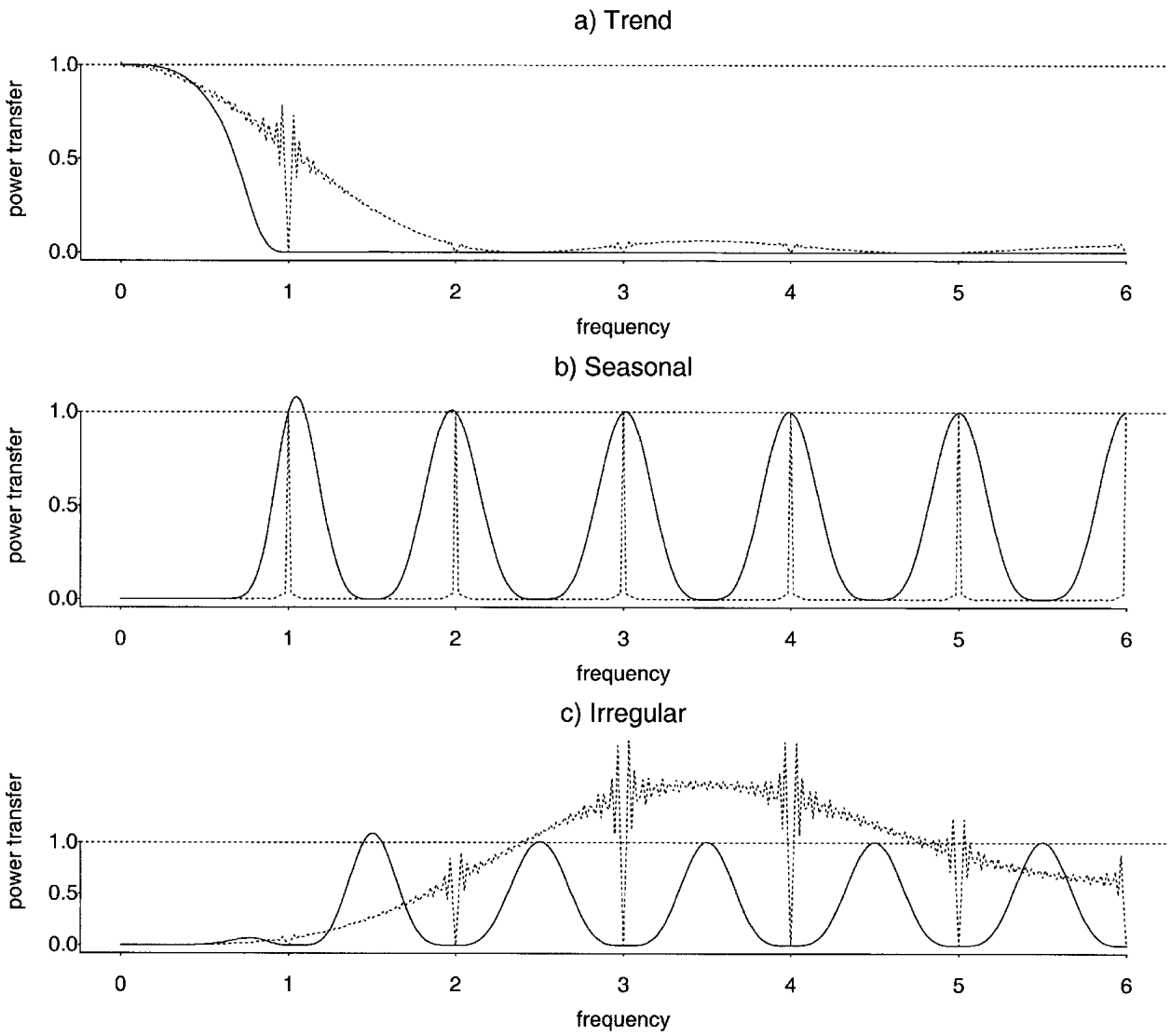

FIG. 1. Spectral power transfer properties of the X-11 approach (solid line) and the traditional approach (dashed line): (a) the trend component, (b) the seasonal component, and (c) the irregular component.

$SMA_{2\times2}$ is based on three consecutive years (with weights 1/4, 1/2, 1/4) and so is *the most local* of the suggested alternatives. Another 3-yr-based filter is the simplest SMA_3 (with weights 1/3, 1/3, 1/3) but the resulting power transfer on S_t would produce secondary peaks on halfway frequencies of the subannual range $f = 1.5, 2.5, \ldots, 5.5$.

In order to extend X-11 to any periodicity p, the filter $MA_{2\times12}$ (appendix B) can be substituted by $MA_{2\times p}$ if p is even and by MA_p otherwise. The Henderson filter length $h = 23$ must also be replaced by $2p - 1$. With these changes, the same spectral properties shown here for monthly data will be achieved in general.

Moving averages cause some terms at the end of the series to be lost. Many methods for the imputation of these lost values have been suggested so far (e.g., see Findley et al. 1998). The simplest one is the circular method, where the last year is replicated until necessary to fill in the gaps. A simple alternative method is the all-available-data method, which consists in giving zero weights to the lost observations when filtering the data. The results shown in this study use the circular method, but no significant differences were found when using the all-available-data method.

3. Data and results

After describing the temperature data used in this study, this section presents some of the results obtained by applying the X-11 procedure and by comparing these findings with the traditional approach.

a. Data

We have used for our analysis various monthly sea surface temperature (SST) indices over the equatorial Pacific and global gridded 2-m air surface temperatures. SST time series include four monthly Niño time indices: Niño-3.4, Niño-1.2, Niño-3, and Niño-4.

The Niño-3.4 index is obtained by averaging the monthly SSTs over the domain (5°S–5°N, 120°W–170°W). The Niño-1.2, Niño-3, and Niño-4 are obtained by averaging the SSTs over (0°–10°S, 80°–90°W), (5°S–5°N, 90°–150°W), and (5°S–5°N, 160°E–150°W), respectively. The SST data used to construct these indices consist of monthly gridded optimum interpolation analyses made at the National Centers for Environmental Prediction (NCEP; the Web site utilized is http://nic.fb4.noaa.gov:80/data/cddb/). The data covers the period January 1950 to February 2002.

The other data consist of the NCEP–National Center for Atmospheric Research (NCEP–NCAR) gridded 2-m air temperature, over the period January 1948 up to February 2002, and were obtained from the Climate Diagnostics Center (CDC; the Web site utilized is http://www.cdc.noaa.gov/cdc/data.ncep.reanalysis.derived.html). The gridded data were provided on a T62 Gaussian grid with spatial resolution 192×94 from 88.542°N–88.542°S and 0°–358.125°E.

b. An example: Niño-3.4 temperatures

The area-averaged SSTs in the Niño-3.4 region (5°S–5°N, 120°E–170°W) of the equatorial Pacific Ocean provide an interesting and important example for demonstrating the X-11 procedure.

Compared to the Niño-3 time series, the Niño-3.4 region has the advantage of being more centrally located in the Pacific and thereby better captures all ENSO events. The Niño-3.4 anomalies are less skewed and more normally distributed than are Niño-3 anomalies, and hence produce a more symmetric and less problematic ENSO index (Burgers and Stephenson 1999; Hannachi et al. 2003). Furthermore, correlation analysis of the Southern Oscillation index (SOI) and SSTs in the eastern equatorial Pacific (e.g., Wang 1995; Trenberth and Hoar 1996) indicate that the key region is somewhat farther west of the Niño-3 region. For these reasons the Niño-3.4 index is increasingly used to define ENSO events instead of the Niño-3 index (Trenberth 1997).

Figure 2a shows a time series plot of X_t (dashed line), the monthly mean Niño-3.4 temperatures from January 1950 to February 2002. One can clearly note the anomalously warm El Niño episodes of 1982/83, 1987/88, and 1997/98, and the anomalously cold La Niña episodes in 1973/74, 1976, and 1988. The time series can be seen to consist of a strong seasonal variation superimposed upon a longer-term interannual variation.

The X-11 procedure was applied to the Niño-3.4 time series to separate out trend, seasonal, and irregular components. The solid line in Fig. 2a shows the resulting trend component, T_t, which clearly picks out the smooth interannual variations in the mean level related to ENSO events. The seasonal component, S_t, shown in Fig. 2b, exhibits strong variation in magnitude throughout the years. For example, since 1999 and from 1990 to 1994, the seasonal component has much greater amplitude than in the remaining periods, for example, 1987/88 and 1995/96. This indicates that the seasonal magnitude is not simply related to ENSO events with, for example, reduced amplitude during El Niño events and increased amplitude during La Niñas. Figure 2c shows the irregular component, I_t, left over after subtracting out the seasonal and trend components from the original time series. The irregular component consists of noisy subannual variations that show no apparent trends. However, some interesting short-term persistence in the irregular component can be seen in certain periods such as 1970–74 and 1994–99.

Figure 3 shows the same time series in matrix representation: image plots of the Niño-3.4 index as a function of year and calendar month. The original time series is shown in Fig. 3a and the corresponding X-11 trend and seasonal components are shown in Figs. 3b and 3c, respectively. The trend component clearly picks up the major ENSO events as tilted vertical bands of persistent values. It can be seen that the strongest amplitudes occur mainly in the cold winter season. Note that only a *single* cold event can be seen after 1998 in the X-11 trend component and this will be discussed in more detail in section 3d. The seasonal component in Fig. 3c shows a strong dependence on calendar month with warmest temperatures generally in April–May and coldest temperatures in November–March. However, there is also a clear variation of the seasonal component from year to year, most likely due to modulation of the SSTs by long-term changes in the depth of the thermocline.

Interannual variation in the seasonal component accounts for a nonnegligible fraction of the total variance of the original Niño-3.4 index. A Monte Carlo procedure can be used to test whether this fraction is larger than could be expected due to chance sampling assuming the null hypothesis of fixed seasonality (see appendix C). For the Niño-3.4 index the interannual variation in seasonality is statistically significant at the 1% level, and so the hypothesis of fixed seasonality can be rejected. This suggests that the traditional approach that assumes fixed seasonality is not appropriate for this index.

For Niño-1.2 and Niño-4, the test obtains the same result at the 1% level. Interestingly, it turns out that this is not the case for the Niño-3 index (p value 0.18), for which the stability of the annual cycle can not be rejected. These results are in agreement with those of Trenberth and Hoar (1996) where ocean–atmosphere interactions were found on the Niño-3.4 rather than the

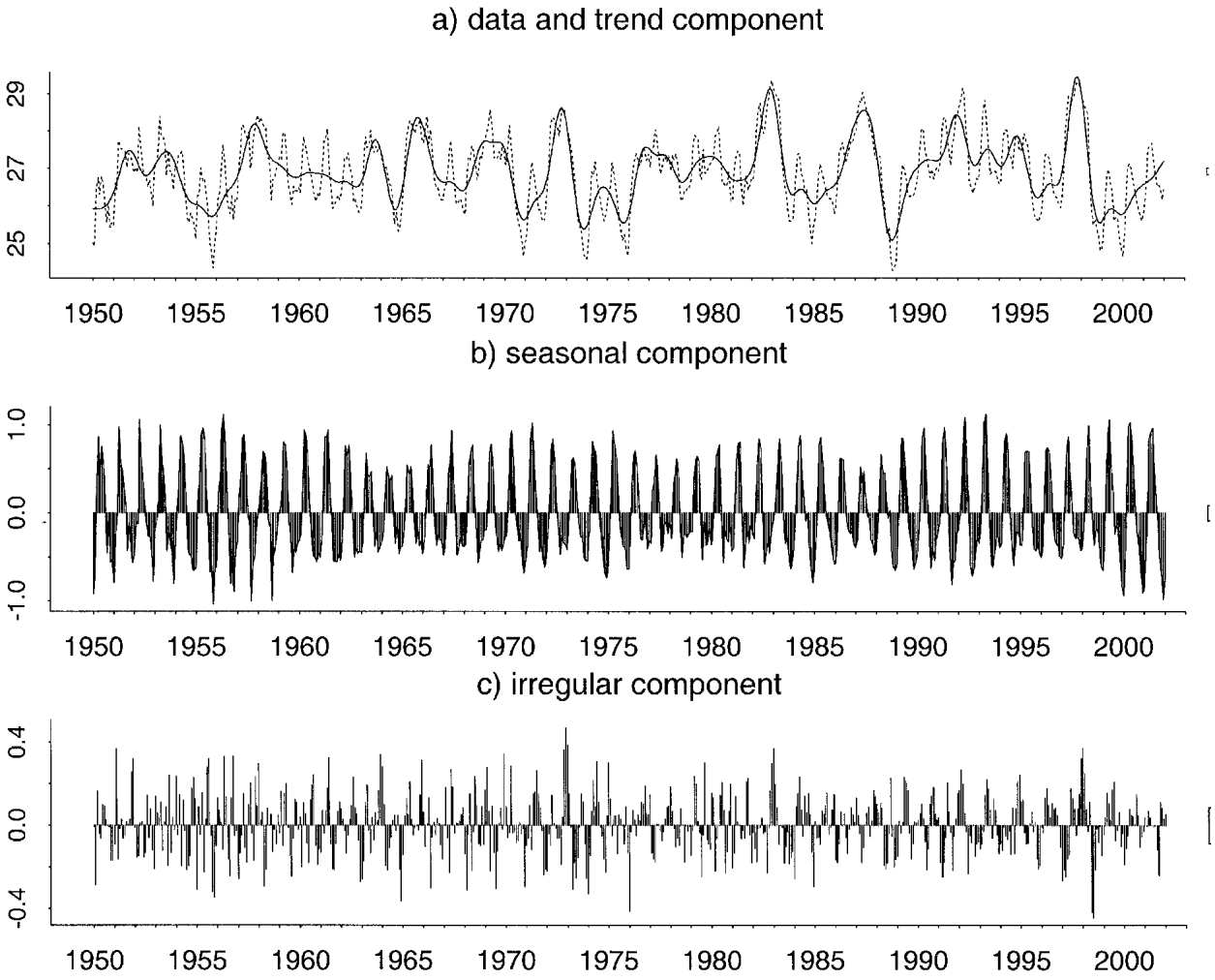

FIG. 2. The X-11 decomposition of the Niño-3.4 SST time series: (a) original series (dashed) and X-11 interannual trend component (solid); (b) X-11 interannually varying seasonal component; and (c) X-11 irregular component. [Note that the vertical scale in (a)–(c) is different—the same interval of 0.2°C is indicated by the vertical bar at the right of each plot.]

Niño-3 region. Because the interaction between various modes of the spectrum can alter the seasonal response to the solar forcing, the most interacting areas are likely to show a variable annual cycle. The tests have been repeated with different Henderson filters (e.g., with larger/smaller spans) and the results were not found to be overly sensitive to the specific choice of filter.

c. Interannually changing seasonality map

To further identify regions with variable seasonality, we have applied the statistical test to global gridded 2-m air surface temperatures. Figure 4 shows the resulting p-value map of the test statistic (appendix C). Dark regions correspond to the smallest p values (less than 1%), that is, regions where there is strong evidence of changing seasonality. Intermediate p values (between 1% and 10%) are shown in lighter gray. White regions (more than 10%) correspond instead to the most regular annual cycles.

There is evidence of significant changes in seasonality over most of the Tropics. Particular key regions for climate interactions include the Indian, the Pacific, and the Atlantic Oceans, and also some extratropical areas such as Antarctica. The results in Fig. 4, are also in agreement with the results obtained by applying the statistical test to the four ENSO indices. For example, unlike the Niño-3.4, the Niño-3 region in Fig. 4 does not show strong evidence of variable seasonality.

d. Improved definition of ENSO events

It is of interest to compare the trend obtained from the traditional definition to the X-11 trend component. Traditionally, ENSO indices are obtained by smoothing anomalies from the mean annual cycle using an arbi-

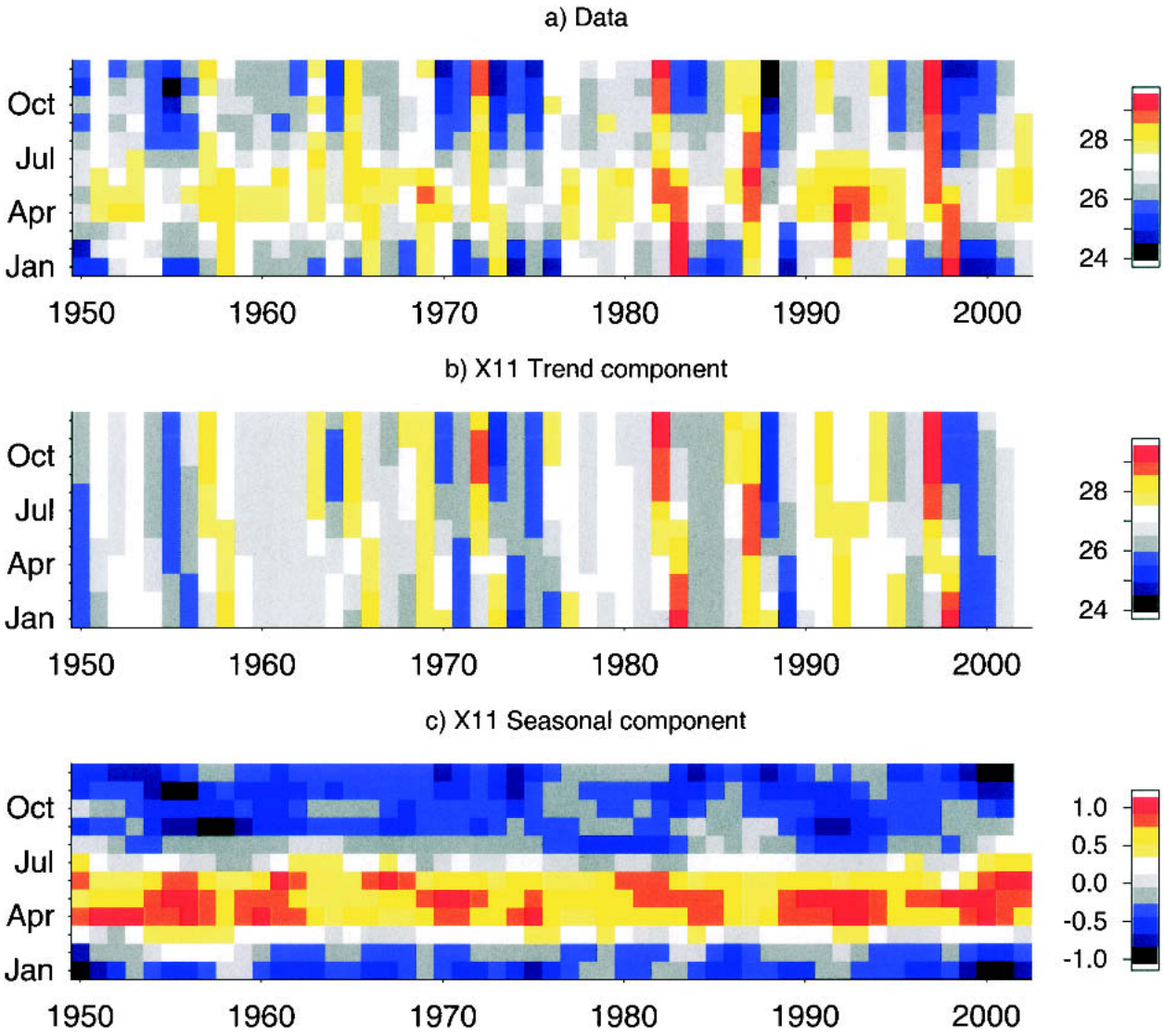

FIG. 3. Matrix two-way representation of Niño-3.4 temperature time series: (a) the original monthly mean data; (b) the X-11 trend component; and (c) the X-11 seasonal component.

trary 5-month moving average A_t^*. Figure 5 shows Niño-3.4 indices defined using both the traditional smoothed anomaly approach (Fig. 5a) and the X-11 (centered) trend approach (Fig. 5b).

Both indices seem to agree broadly with one another. However, more careful inspection reveals that the X-11 trend yields a smoother index with less short-term variations. For example, the traditional approach shows a series of small ripples during 1983–86 and 1998–2002, which are much less evident in the X-11 trend component. By the traditional index the ripples shown in Fig. 5a since 1998 are interpreted as a series of La Niña events. The X-11 interpretation, instead, suggests a simpler single and more reasonable (because it is more consistent with ocean dynamics) La Niña event starting in 1998.

The reduction in short-term variations is not simply due to different amounts of smoothing in the two approaches, since it can be seen that the X-11 trend is also able to correctly reproduce the peak amplitudes associated with the major ENSO events.

Figure 5c shows the difference between traditional and X-11 indices. Since the former assumes a fixed annual cycle, the interannual variations of seasonality are split between the trend index A_t^* and the residual irregular component R_t^*. However, as has been pointed out from the spectral analysis of the traditional approach in section 2c, most of the variable-seasonality signal is likely to be falsely "explained" by the interannual trend component (the five-term running mean). The difference between the two index definitions (Fig. 5c) shows many 1-yr cycles caused by variations in the annual cycle.

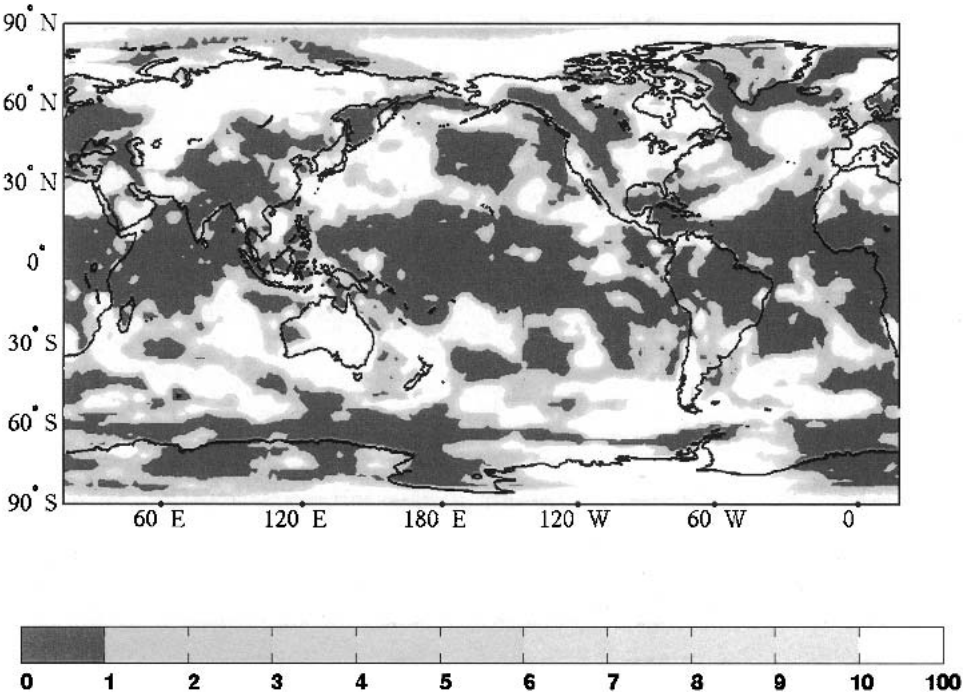

FIG. 4. The p values (%) of the fixed seasonality test [in case of independent heteroscedastic irregular terms (see appendix C)], applied to the gridded 2-m air surface temperatures.

Figure 6 shows time–longitude plots of sea surface temperatures in the equatorial Pacific since 1994. The evolution of the traditional 5-month running mean anomalies (Fig. 5a) and the centered X-11 trend (Fig. 5b) are quite similar up until just after the El Niño event in 1998. After 1998, the traditional approach gives the impression that there are three separate westward-propagating La Niña events whereas the X-11 trend gives a much simpler picture of just one single extended La Niña event lasting from mid-1998 until end of 2000. The reason for the different interpretation can be clearly seen in the increased amplitude of the seasonal component in Fig. 5c that occurred after 1999. The change in the annual cycle translates into a misleading impression of multiple La Niña events when viewed from the traditional approach perspective. The extended nature of the cold event can also be confirmed by careful diagnosis of multiple variables (Lawrimore et al. 2001). Possible mechanisms for the extended nature of the ENSO event include multidecadal modes in the tropical Pacific (Chelliah and Bell 2004; Vimont et al. 2002) and phase-locked interaction with the Asian monsoon (Kirtman and Shukla 2000).

In summary, the assumption of fixed seasonality in the traditional approach leads to ENSO indices that contain variations in seasonality in addition to smooth interannual trends. The centered X-11 trend avoids confounding changes in seasonality with interannual trends, and therefore can provide a more reliable index for defining ENSO events.

e. Interannual volatility

A simple and widely used measure of variability is provided by the standard deviation s_X of the time series X_t. On the other hand, the contribution from year-to-year variability can be assessed by considering the standard deviation $s_{\Delta X}$ of the 12-month differences $\Delta X_t = X_t - X_{t-12}$ in the monthly mean time series. Twelve-month differencing is a simple well-known method for detrending time series that removes both the mean annual cycle and the linear trend. We will refer to this quantity as the *volatility* of X, since it represents the typical size of innovations from one year to the next.

Small volatility, relative to s_X, is an indication that the 12-month-ahead persistence forecasts, $\hat{X}_{t+12} = X_t$, provide good predictions of future values. In fact s_X can be interpreted as the root-mean-square error of predicting the time series using climatology, whereas $s_{\Delta X}$ is the root-mean-square error in predicting the same observations using the previous year data. A small ratio $s_{\Delta X}/s_X$ indicates that *persistence forecasts* will give good results, compared to the general uncertainty in the data.

Figure 7a shows a map of the standard deviation $s_{\Delta X}$ of year-to-year differences, that is, volatility, in monthly mean 2-m air temperatures. The largest volatility occurs at high latitudes near the edge of sea ice and over continental regions. Small changes in the position of sea ice or snow cover from one year to the next can easily lead to large changes in surface air temperature. Less volatility can be seen over the oceans, although the

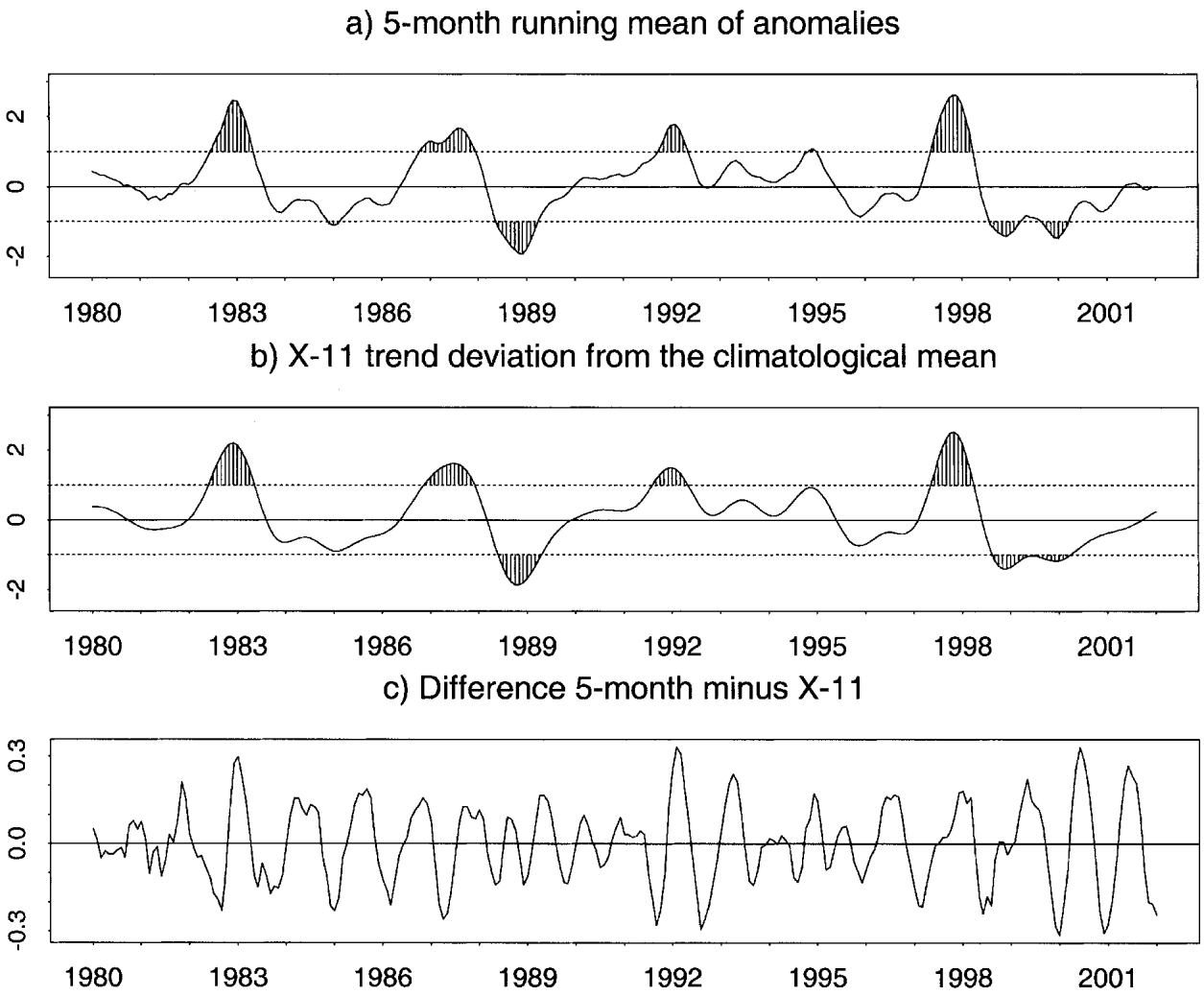

FIG. 5. Niño-3.4 sea surface temperature anomalies from 1980 to 2002: (a) traditional 5-month running mean anomalies and (b) centered X-11 trend component. Note the smoother evolution of the X-11 anomalies that could be used to construct a less ambiguous index for defining El Niño and La Niña events. (c) The difference between (a) and (b).

characteristic ENSO upwelling region in the eastern equatorial Pacific associated with ENSO can also be noticed.

Let us consider the decomposition $\Delta X_t = \Delta S_t + \Delta \mathrm{N}_t$, where $N_t = T_t + I_t$ is the nonseasonal (aggregate) component. Hence we obtain the squared-volatility decomposition:

$$s^2_{\Delta X} = s^2_{\Delta S} + s^2_{\Delta N} + 2s_{\Delta S,\Delta N},$$

where $s_{\Delta S,\Delta \mathrm{N}}$ is the covariance between seasonal and nonseasonal components.

The main point is that, by using a variable-seasonality approach, one can potentially predict the interannual variations in both seasonal and nonseasonal components, while the traditional approach, by definition, can only address the nonseasonal variability. Thus, a measure of the gain in 1-yr-ahead predictability, allowed by nontraditional variable-seasonality methods, is the seasonal volatility $s_{\Delta S}$. Note that this ignores the interaction between seasonal and nonseasonal components that is represented by the covariance term in the preceding squared volatility decomposition.

The seasonal volatility $s_{\Delta S}$ is shown in Fig. 7b. In comparing this map with the total volatility map of Fig. 7a, we note a very similar pattern, although the ENSO upwelling region is not visible anymore, and the scale is reduced by about a third. Finally, the relative seasonal volatility $s_{\Delta S}/s_{\Delta X}$ is shown in Fig. 7c. Around 24%–40% of the total volatility over land regions is due to year-to-year changes in the seasonal component. Because of its slow variation, this component is potentially predictable and represents a window of opportunity for improving seasonal climate forecasts. Over the tropical Pacific and Atlantic Oceans less volatility is accounted for by the seasonal component, most likely due to the

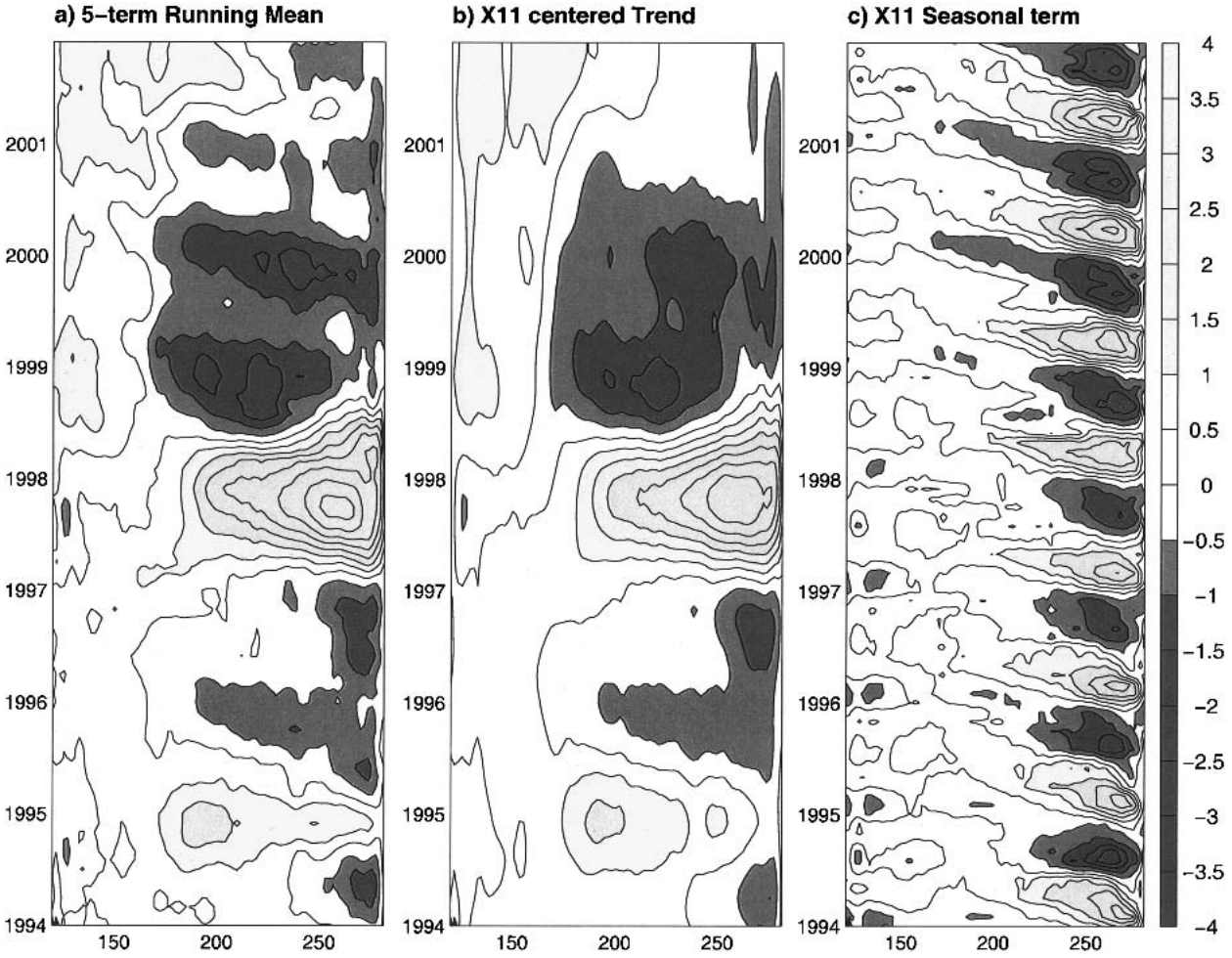

FIG. 6. Time–longitude plot of SSTs in the equatorial Pacific Ocean from 1994 to 2002: (a) traditional 5-month running mean anomalies; (b) centered X-11 trend component; and (c) the X-11 seasonal component. Note in (a) the three apparent La Niña events since 1999 and their reduction in (b) and the marked increase in seasonal amplitudes after 1999.

dominance of the trend component. However, even in these tropical regions, the seasonal component accounts for more than 10% of the total volatility.

f. Global teleconnections

It is well known that there exist significant correlations between climatic variables calculated at locations separated by large distances. These *teleconnections* are a major component of climate variability and their study can provide a deeper understanding of the climate system. This section will present an interesting example of the teleconnections that exist in the trend and seasonal components of 2-m air temperature.

Figure 8a shows the correlation map of the center of the Niño-3.4 region (0°, 145°W) with elsewhere, for the monthly mean X-11 trend component in 2-m air temperature. The characteristic boomerang-shaped ENSO pattern can be clearly seen in the Pacific Ocean, where positive correlations are found over a large area centered over the Niño-3.4 region, but also extending along the western coast of both North and South America. Positive correlations with the western tropical Indian Ocean are found. Regions whose trend is negatively correlated with the Niño-3.4 trend are indicated by dotted contours. Negatively correlated areas are also rather large and form a typical wave train pattern with positively correlated areas.

Figure 8b shows a similar one-point Niño-3.4 correlation map, using instead the 12-month running means of the modulus of the seasonal component. In other words, Fig. 8b shows teleconnections between interannual variations in seasonal amplitudes around the globe and seasonal amplitudes in the Niño-3.4 region. Compared to Fig. 8a, teleconnections in seasonal amplitudes appear to be far more extended over the globe, than are the teleconnections in the trend component. Although positive correlations in the equatorial Pacific cover a somewhat smaller region than in Fig. 8a, there are more extended teleconnections over both the Atlantic Ocean

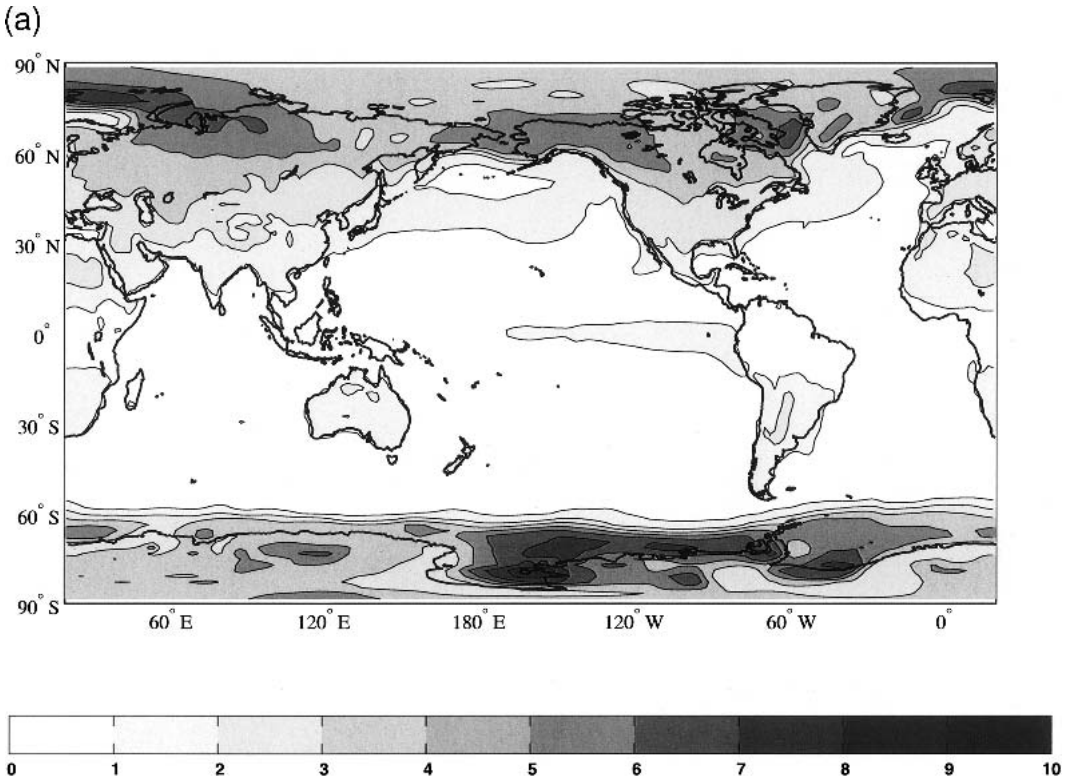

FIG. 7. Maps of interannual variations in surface temperatures: (a) standard deviation $s_{\Delta X}$ of year-to-year differences in monthly mean 2-m air temperatures (data volatilities); (b) seasonal volatilities $s_{\Delta S}$; and (c) fraction of variation $s_{\Delta S}/s_{\Delta X}$ (%) due to interannual variations in the X-11 seasonal component.

and Africa. Negative correlations over both North and South Poles are also found. Teleconnections in seasonality suggests possible opportunities for improving seasonal climate forecasts outside the Tropics.

These types of teleconnection in seasonal amplitude rather than in the long-term mean are intriguing and merit further investigation beyond the scope of this study. For example, cross correlations within trend, seasonal and irregular components, different fixed points, and different time lags could also be studied.

4. Conclusions

Seasonal variation is one of the most noticeable and dominant aspects of climate variability. Despite external solar forcing being (almost) perfectly periodic, there is no fundamental reason why the seasonal climate response should remain exactly the same from year to year. The traditional approach assumes a fixed annual cycle response, which is appropriate only if the solar forcing is perfectly periodic and there are no nonlinearities or internal modes of variability. Under these assumptions, variability is simply the sum of internal variability and the response to the external forcing. However, the observational evidence presented here and in previous studies (cited in the introduction) suggests that annual cycles in temperature vary from year to year. The traditional approach has the disadvantage that variations in seasonal behavior become mixed up with longer-term interannual variations in the mean. As mentioned in the introduction, well-known nonlinear phenomena such as phaselocking can produce simultaneous quasi-seasonal frequencies, and lead to changing seasonality. Longer-term variability of internal modes of the climate system such as ENSO and climate change can also easily modulate the climate system's response to periodic solar forcing. Some understanding of how these nonlinearities may affect variations in seasonality could be gained by modeling studies of periodically forced low-order chaos models (e.g., Lorenz 1963).

Seasonality is not uniquely defined—it depends on which method is used to isolate the seasonal component. Different methods make different underlying assumptions and reveal different aspects of seasonality. Empirical approaches such as the X-11 method used here and complex demodulation (Bloomfield 1976; Thompson 1995) use predefined filters to extract, in a flexible manner, the varying seasonal component. However, a more explicit structural approach to seasonality is to use a (suitable) time series model to extract the various components. Autoregressive time series models can be used such as the seasonal ARIMA models

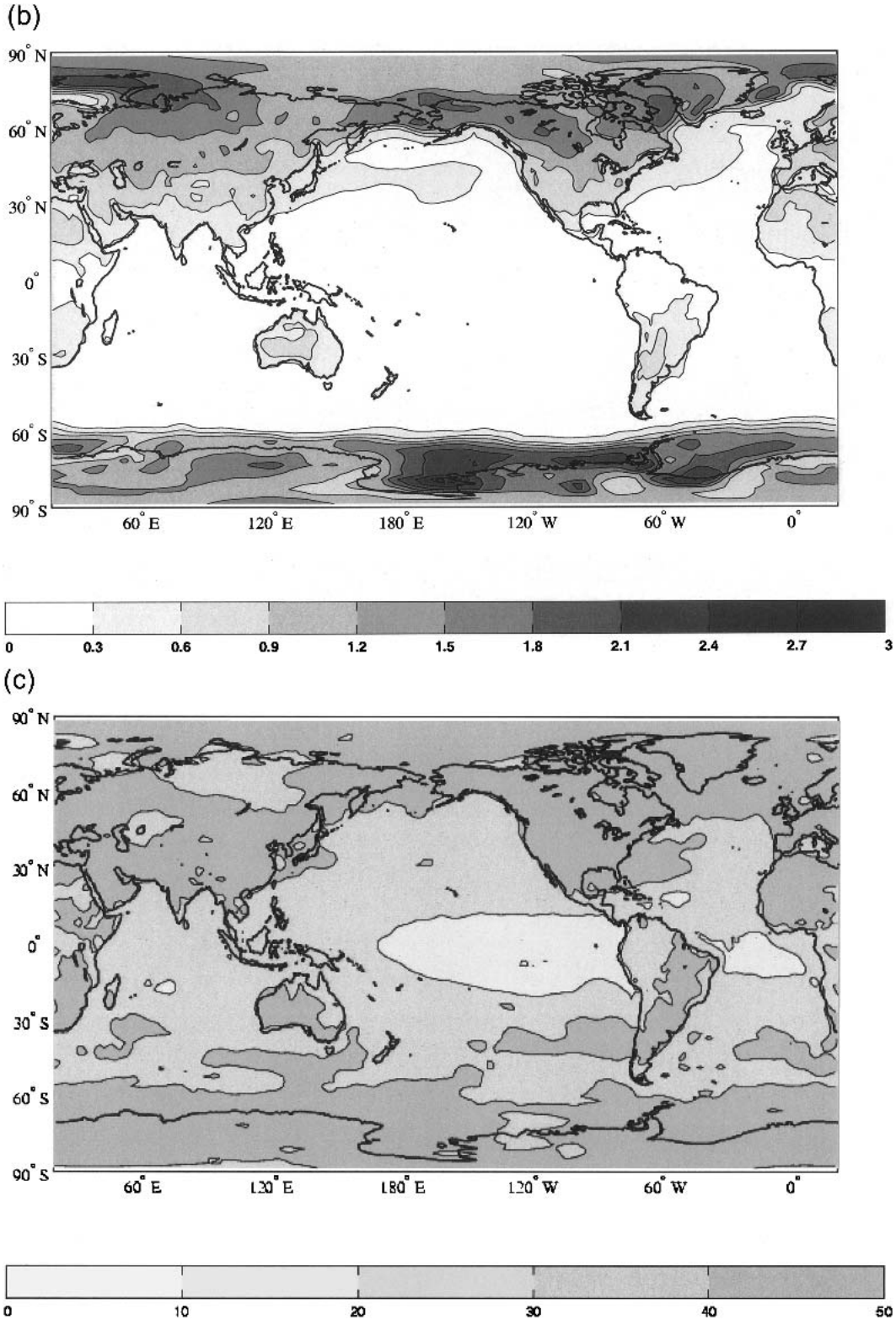

FIG. 7. (*Continued*)

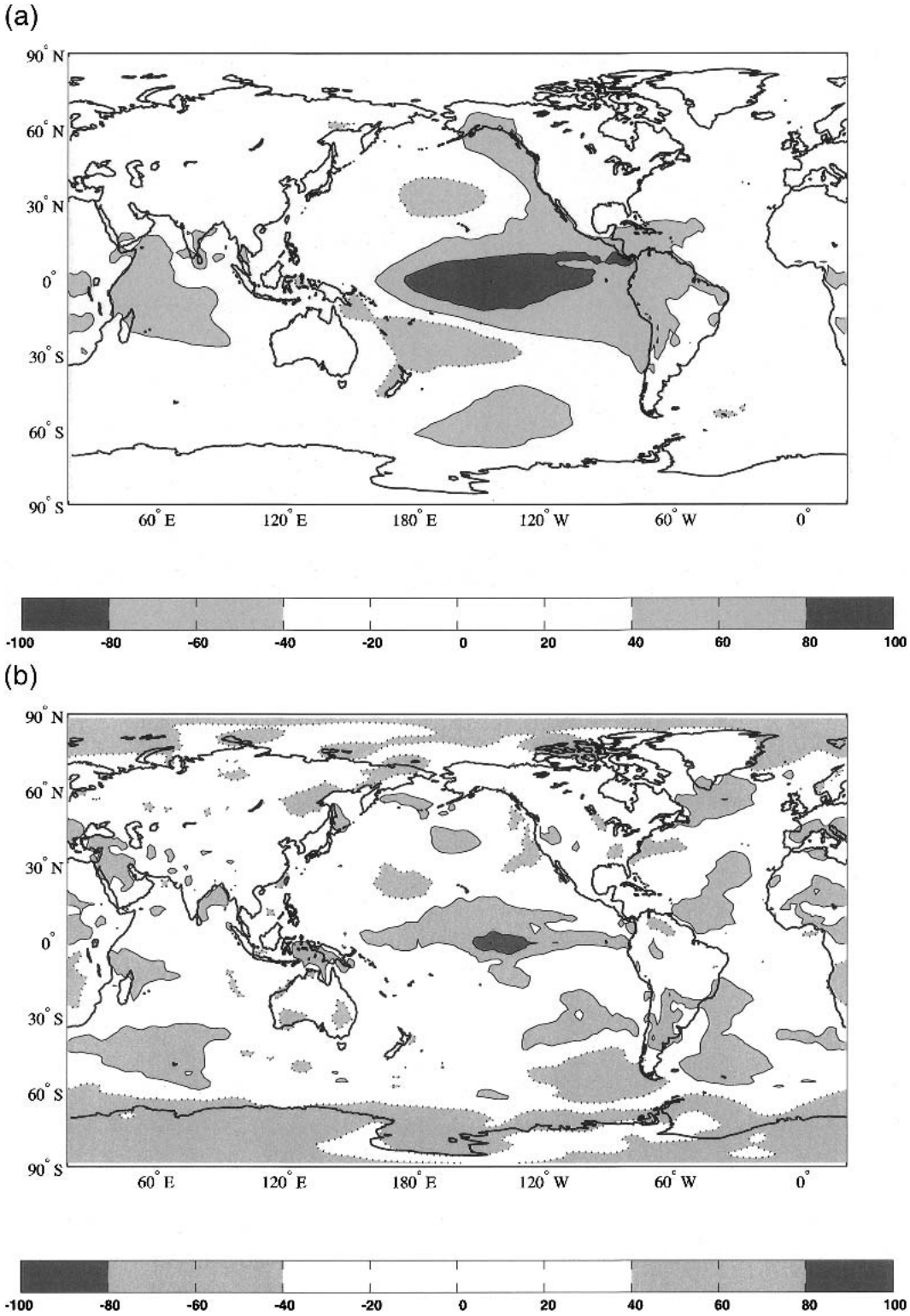

FIG. 8. Correlation maps showing teleconnections of monthly mean 2-m air temperatures with the Niño-3.4 region: (a) correlation between trend components and (b) correlation between seasonal amplitudes.

or the periodic ARIMA models (Franses 1996). Periodic ARIMA models have been shown to be useful for describing and predicting time series having *periodic correlations,* in other words time series whose autocorrelations are stationary with respect to time translations by multiples of one period (Lund et al. 1995). Such time series are also known as *cyclostationary* time series (Huang and North 1996, and references therein). A more holistic model-based approach is to treat the annual cycle as a smooth function of calendar month and then use an autoregressive approach to forecast the whole function in the following year (Besse et al. 2000).

In this study, we have presented a simple approach based on the X-11 procedure for analyzing seasonal variations. By relaxing the strong assumption of a fixed annual cycle, the annual cycle is treated as a fundamental entity on its own and can then be studied in more detail. The X-11 approach defines the seasonal component using filters that are local in time, whereas the traditional approach relies on averaging over all years in the sample. This local property ensures that the values obtained in any one year are not overly biased by events happening at other times that could be unrelated to events in that year. For example, an unusually large El Niño event such as 1982/83 can easily bias all other years in the traditional approach. Local behavior also guarantees that spectral transfer properties do not depend on the length of the record, which is not the case for the traditional approach. For shorter records, the traditional approach provides less reliable estimates of the mean annual cycle and distinguishes less well between interannual and annual cycle variations. The main advantage of X-11 is that it is able to cope with changes in the annual cycle whereas the traditional approach assumes that such changes do not happen. For example, when applied to the Niño-3.4 index, it has been shown that the X-11 approach clearly takes account of the recent increase in Niño-3.4 seasonal amplitude, whereas the traditional approach suggests instead occurrence of spurious multiple La Niña events. The X-11 approach has the flexibility to deal with changes in seasonality expected from natural variability and anthropogenic climate change. It may also be of use in paleoclimate studies, where variations in seasonality are of great interest (Clement et al. 1999; An et al. 2000; Rutherford and D'Hondt 2000; Koutavas et al. 2002).

Our conclusions are robust and not overly dependent on the choice of dataset. The X-11 results from the NCEP–NCAR 2-m temperature analyses agree well with those of the Nino indices based on the Reynolds SST dataset. Furthermore, we have also applied X-11 to the Southern Oscillation sea level pressure index and found similar conclusions concerning the nature of the La Niña events after 1998 (not shown). The NCEP–NCAR reanalyses have a known problem with the 2-m air temperature associated with the skin temperature when the wind is weak (less than about 0.75 m s^{-1}). We have inspected the NCEP–NCAR wind speeds and found that the regions where the wind speed is smaller than 0.75 m s^{-1} are concentrated in a very narrow band over mountainous regions in central Africa and the Andes (less than 2% of the globe). Furthermore, the skin temperature problem is much less of an issue when dealing with monthly and seasonal means rather than daily data (Chelliah and Bell 2004). We feel confident that similar results would be obtained using other surface temperature datasets.

As in economics, the X-11 approach is able to seasonally adjust time series so that the resulting trend component correctly reflects long-term changes in the mean level of the process. Therefore, the X-11 trend component is able to produce better climate indices for monitoring and predicting interannual and longer-term climate variations, and this has been demonstrated with the Niño-3.4 index. Similarly, we have shown using the volatility maps that a substantial fraction of year-to-year variation over land areas is due to interannual variation in the seasonal component. Further, we demonstrated that teleconnections can also be found between the annual cycle amplitudes. These findings indicate some potential for improving seasonal forecasts. The understanding of the variations in the annual cycle is particularly important for applications in agriculture.

In conclusion, we believe that the traditional approach based on the assumption of a fixed annual cycle is unjustifiable on physical grounds and is overly restrictive. Relaxing this assumption using procedures such as X-11 (and complex modulation, etc.) can lead to a richer diagnosis and clearer interpretation of climate variations. Obvious extensions would be to use the X-11 method to understand and validate output from climate model simulations and seasonal forecasts. The X-11 approach could also be of use in analyzing other quasi-periodic phenomena such as the diurnal cycle.

Acknowledgments. We wish to thank Tara Ansell, Emily Black, Chris Ferro, and Julia Slingo for stimulating discussions concerning this work.

APPENDIX A

The Two-Way ANOVA Model

Equation (1) defines an additive decomposition of the data into a constant mean μ, a periodic seasonal effect $\tilde{C}_t$, a piecewise constant trend A_t and a residual short-term error component R_t. This model is called the *two-way* ANOVA model in statistical literature (see, e.g., Cressie 1991) and it is elegantly summarized in matrix form as

$$x_{my} = \mu + \tilde{c}_m + a_y + r_{my}. \quad \text{(A1)}$$

In a two-way model, apart from the residual term r_{my}, data variation occur as a row variation (an annual effect) and/or as a column variation (seasonal effect). In

fact, the effect of annual and monthly factors is easiest to interpret if their joint contribution is the sum of two separate contributions.

The least squares fit is optimal in various theoretical senses when the residuals have an underlying distribution with certain special properties. For example, it is often assumed that the r_{ma} are fluctuations independently and normally distributed with zero mean and constant variance, but it is still asymptotically optimal when the residual variance can vary (e.g., with the seasonal index m).

The least squares fit of the two-way model is performed by finding and subtracting row and column means. We could begin with the mean of all the values in the table to estimate μ, and then subtract it from all observations. Next, we could calculate the mean of each column for the annual (net) contribution, a_y, subtract it from every observation in the column and, finally, estimate $\tilde{c}_m$ by the row means of these residuals. Alternatively, as in section 2a, we can proceed by rows and obtain first the monthly effects $\tilde{c}_m$ (by centering the monthly averages c_m) and then the annual effects by the annual means of the anomalies. The results are invariant because of the properties of the arithmetic mean, and successive iterations on the residual matrix would find no further row and column contributions.

The recursive definition of X-11, given in section 2b, can be seen to be a very simple extension of this process, starting from trend (column) subtraction. In order to obtain a continuous trend, the running annual mean (on the starting step) and the Henderson filter (on steps 2 and 3) replace the (yearly constant) annual mean and the local seasonal filter replaces the annual cycle (the seasonal mean filter) to obtain quasi-periodic seasonality.

APPENDIX B

Trend and Seasonal Filters

Note that the symbol MA_m, defined in section 2 for the five-term running mean ($m = 5$) is ambiguous when the index m is even. In this case it can allow two definitions. For example, for $\mathrm{MA}_2(X_t)$ one can choose between $(X_{t-1} + X_t)/2$ and $(X_t + X_{t+1})/2$. The means of these two is called the *centered* running mean and denoted, in general, as $\mathrm{MA}_{2\times m}$. Two relevant examples are the two-term centered filter

$$\mathrm{MA}_{2\times 2}(X_t) = \frac{X_{t-1} + 2X_t + X_{t+1}}{4}$$

and the annual centered filter

$$\mathrm{MA}_{2\times 12}(X_t) = \frac{X_{t-6} + 2X_{t-5} + \cdots + 2X_t + \cdots + 2X_{t+5} + X_{t+6}}{24}.$$

Both the MA_m, when m is odd, and the $\mathrm{MA}_{2\times m}$, when m is even, are centered averages, or symmetric filters, because they rely on an odd number of consecutive terms and have symmetrical weights $\alpha_j = \alpha_{-j}$. A (finite) symmetric filter of an input series X_t produces an output F_t of the form

$$F_t = \sum_{j=-m}^{m} \alpha_j X_{t+j} = \alpha_0 X_t + \sum_{j=1}^{m} \alpha_j (X_{t-j} + X_{t+j}).$$

A seasonal running mean SMA is obtained by separate applications of the MA on each seasonal subseries. For example, on monthly data, the series $\mathrm{SMA}(X_t) = F_t$, with matrix form $\mathbf{F} = \mathbf{f}_{\mathrm{am}}$, is given by filtering with MA the January subseries $\{X_1, X_{13}, X_{25}, \ldots\}$ to fill the first column (f_{a1}), then the February subseries $\{X_2, X_{14}, X_{26}, \ldots\}$ giving the f_{a2} values, and so on. Seasonal moving averages based on symmetric filters are symmetric filters as well.

The fixed seasonal series C_t, on the other hand, can be seen as an infinite symmetric filter, because it is equivalent to an SMA_{2m+1} when the semiwindow parameter m of the filter tends to infinity, since in this case

$$\mathrm{SMA}_{2m+1}(X_t) \to C_t. \tag{B1}$$

In practice, this causes distortion effects on short climatological time series (see Fuenzalida and Rosenblüth 1986).

APPENDIX C

Testing Fixed Seasonality

From initial data analysis, temperatures appear to be well fitted by the additive model, either the traditional or the X-11 decomposition. The main difference is that a global or a local seasonal filter is being used.

The next question is whether or not the traditional assumption of fixed seasonality can be accepted. Let us call H_0 the traditional hypothesis. Several tests for the presence of variable seasonality have been developed. The early version of X-11 included an F test based on a two-way analysis of variance performed on the detrended data developed by Higghinson (1975). Other tests were introduced later by Dagum (1978), Findley et al. (1990), and Sutradhar and Dagum (1998). The main problem of these approaches is that easy versions are incorrectly based on the F distribution, so that the *nominal* significance level is not the actual one. More accurate procedures, instead, relying on the actual distribution of the test statistic, are quite complicated in computing both the statistic and the significance level, and so these are not well suited for testing gridded climate datasets.

Monte Carlo (MC) testing, on the other hand, allows an exact control of the significance level. Therefore, a relatively simple MC method is proposed

here to verify the fixed seasonality assumption H_0 against the alternative of a moving seasonality characterized by gradual changes in the seasonal amplitudes, as estimated by X-11. As usual it will be assumed that the trend can be well estimated by the X-11 trend filter T_t. Alternatively, the 13-term running mean can be used (Sutradhar and Dagum 1998).

Given a time series X_t with fixed net cycle $\tilde{C}_t$ and X-11 trend T_t, let σ_m^2 be the seasonal variances of the residual terms

$$V_t = X_t - T_t - \tilde{C}_t.$$

Let σ_t^2, $t = 1, 2, \ldots,$ N be the periodic extension of these p variances for the entire length of the time series. The MC test is as follows:

(a) generate a large number of samples

$$X_t^* = T_t + \tilde{C}_t + W_t^*,$$

where T_t and $\tilde{C}_t$ are always the same series, as estimated on the original data, while the irregular terms

$$W_t^* \sim N(0, \sigma_t^2) \qquad \text{(C1)}$$

(which means that they are drawn from a normal distribution with mean zero and variance σ_t^2).

(b) Compute the X-11 decomposition of the MC sample

$$X_t^* = T_t^* + S_t^* + I_t^*$$

and the traditional annual cycle $\tilde{C}_t^*$ on the detrended series $X_t^* - T_t^*$. This gives the traditional decomposition (conditional to X-11 trend)

$$X_t^* = T_t^* + \tilde{C}_t^* + V_t^*$$

where the irregular terms V_t^* are the residual series after trend and seasonal subtraction.

(c) On each MC sample, compute and save a test statistic U^*, to be compared with the same statistic U observed on the original data.

At the end, the fraction p^* of U^* that are bigger than U can be used to evaluate the p value for H_0, within a fixed error. More precisely, if m^* is the MC sample size (that is the number of generated samples), then a 95% confidence interval for the p value can be approximated by $(p - 2h, p + 2h)$, where $h = \sqrt{p^*(1 - p^*)/m^*}$.

Any statistic can be used in step c, so long as it is useful to distinguish between fixed and variable seasonality. A classical choice is the F statistic, measuring the lack of fit due to the null hypothesis H_0. Because the residual variability (σ_t) can vary under H_0, the statistic can be written as

$$F^* = \frac{\sum (V_t^*/\sigma_t)^2}{\sum (I_t^*/\sigma_t)^2} - 1.$$

For the current application, on the other hand, another interesting choice is based on the $L1$ distance between the fixed and variable annual cycle:

$$D^* = \frac{1}{N} \sum_{t=1}^{N} (|\tilde{C}_t^* - S_t^*|),$$

which measures, on the MC (simulated) sample X_t^*, the average absolute variation in the original units (e.g., degrees Celsius) between traditional and X-11 seasonal terms.

The stochastic model used in (a) to generate the MC time series with fixed (e.g., exactly periodic) seasonality can be called the null hypothesis model. A significant p value means that the H_0 model is not able to reproduce the observed data and thus H_0 can be rejected. Of course, the more flexible the null model, the more confidence can be put on the rejection. That is why the residual variances σ_t^2 are allowed to vary in (C1) (*heteroscedasticity*).

The null hypothesis was also modeled assuming a Markov process for the irregular component. For this alternative test, the first-order autoregressive [AR(1)] process is fitted to the observed irregular component V_t. Then the MC sampling procedure is accordingly modified: the V_t^* are sampled from the fitted autoregressive process. The remaining part of the procedure remain unmodified.

Since the Markov AR(1) model is more flexible than the uncorrelated AR(0) model, a slight preference for H_0 was generally obtained in performing the MC test by using the former assumption. However, this was not enough to change the test results on El Niño indices. Also the test on the gridded 2-m air temperatures gives small differences and the general conclusions from the p-value map remains unchanged.

Unlike the choice of the error model (Markovian or uncorrelated), the Monte Carlo test is rather sensitive to the choice of the test statistic, F^* or D^*. In general, the D^* statistic obtained more significant p values than the F statistic. The corresponding map of the p values identifies essentially the same regions with unstable seasonality, but with much bigger extensions than the ones found in Fig. 4 for the F statistics.

REFERENCES

An, Z. S., S. C. Porter, J. E. Kutzbach, X. H. Wu, S. M. Wang, X. D. Liu, X. Q. Li, and W. J. Zhou, 2000: Asynchronous Holocene optimum of the east Asian monsoon. *Quat. Sci. Rev.,* **19,** 743–762.

Besse, P. C., H. Cardot, and D. B. Stephenson, 2000: Autoregressive forecasting of some functional climatic variations. *Scand. J. Stat.,* **27,** 673–687.

Bloomfield, P., 1976: *Fourier Analysis of Time Series: An Introduction.* Wiley, 258 pp.

Bograd, S., F. Schwing, R. Mendelssohn, and P. Green-Jessen, 2002: On the changing seasonality over the North Pacific. *Geophys. Res. Lett.,* **29,** 1333, doi:10.1029/2001GL013790.

Burgers, G., and D. B. Stephenson, 1999: The "normality" of El Niño. *Geophys. Res. Lett.,* **26,** 1027–1030.

Chang, P., J. Link, B. Wang, and T. Li, 1995: Interactions between the seasonal cycle and El Niño–Southern Oscillation in an intermediate coupled ocean–atmosphere model. *J. Atmos. Sci.,* **52,** 2353–2372.

Chelliah, M., and G. D. Bell, 2004: Tropical multidecadal and interannual climate variability in the NCEP–NCAR reanalysis. *J. Climate,* **17,** 1777–1803.

Clement, A. C., R. Seager, and M. A. Cane, 1999: Orbital controls on the El Nino/Southern Oscillation and the tropical climate. *Paleocenography,* **14,** 441–456.

Cook, E. R., D. D. Rosanne, J. E. Cole, D. W. Stable, and R. Villalba, 2000: Tree-ring records of past ENSO variability and forcing. *El Niño and the Southern Oscillation: Multiscale Variability and Global and Regional Impacts,* H. F. Diaz and V. Markgraf, Eds., Cambridge University Press, 297–323.

Cressie, N. A. C., 1991: *Statistics for Spatial Data.* Wiley, 900 pp.

Dagum, E. B., 1978: Modelling, forecasting and seasonally adjusting economic time series with the X-11 ARIMA method. *Statistician,* **27,** 203–216.

Findley, D. F., B. C. Monsell, H. B. Shulman, and M. G. Pugh, 1990: Sliding span diagnostics for seasonal and related adjustments. *J. Amer. Stat. Assoc.,* **85,** 345–355.

——, ——, W. R. Bell, M. C. Otto, and C. Bor-Chung, 1998: New capabilities and methods of the X-11-ARIMA seasonal adjustment programme (with discussion). *J. Bus. Econ. Stat.,* **16,** 122–177.

Franses, P. H., 1996: *Periodicity and Stochastic Trends in Economic Time Series.* Oxford University Press, 230 pp.

Fuenzalida, H., and B. Rosenblüth, 1986: Distortion effects of the anomaly method of removing seasonal or diurnal variations from climatological time series. *J. Climate Appl. Meteor.,* **25,** 728–731.

Gu, D. F., and S. G. H. Philander, 1995: Secular changes of annual and interannual variability in the Tropics during the past century. *J. Climate,* **8,** 864–876.

——, ——, and M. J. McPhaden, 1997: The seasonal cycle and its modulation in the eastern tropical Pacific Ocean. *J. Phys. Oceanogr.,* **27,** 2209–2218.

Hannachi, A., D. B. Stephenson, and K. R. Sperber, 2003: Probability-based methods for quantifying nonlinearity in the ENSO. *Climate Dyn.,* **20,** 241–256.

Henderson, R., 1916: Note on graduation by adjusted average. *Trans. Amer. Soc. Actuaries,* **17,** 43–48.

Higghinson, J., 1975. An F-test for the presence of moving seasonality when using Census Method II X-11 variant. Research paper, Seasonal Adjustment and Time Series Staff, Statistics Canada, 46 pp.

Huang, J.-P., and G. North, 1996: Cyclic spectral analysis of fluctuations in a GCM simulation. *J. Atmos. Sci.,* **53,** 370–379.

Jiang, N., J. D. Neelin, and M. Ghil, 1995: Quasi-quadrennial and quasi-biennial variability in the equatorial Pacific. *Climate Dyn.,* **12,** 101–112.

Jin, F., J. D. Neelin, and M. Ghil, 1994: El Niño on the devil's staircase: Annual subharmonics steps to chaos. *Science,* **264,** 70–72.

——, ——, and ——, 1996: El Niño/Southern Oscillation and the annual cycle: Subharmonic frequency-locking and aperiodicity. *Physica D,* **98,** 442–465.

Kirtman, B. P., and J. Shukla, 2000: Influence of the Indian summer monsoon on ENSO. *Quart. J. Roy. Meteor. Soc.,* **126,** 213–239.

Koutavas, A., J. Lynch-Stieglitz, T. M. Marchitto, and J. P. Sachs, 2002: El Nino-like pattern in ice age tropical Pacific sea surface temperature. *Science,* **297,** 226–230.

Lawrimore, J. H., and Coauthors, 2001: Climate assessment for 2000. *Bull. Amer. Meteor. Soc.,* **82,** 1–55.

Lorenz, E. N., 1963: Deterministic nonperiodic flow. *J. Atmos. Sci.,* **20,** 130–141.

Lund, R., H. Hurd, P. Bloomfield, and R. Smith, 1995: Climatological time series with periodic correlations. *J. Climate,* **8,** 2787–2809.

Meyers, G., 1982: Interannual variation in sea level near Truk Island—A bimodal seasonal cycle. *J. Phys. Oceanogr.,* **12,** 1161–1168.

Philander, S. G. H., 1990: *El Niño, La Niña, and the Southern Oscillation.* Academic Press, 293 pp.

Rasmusson, E. M., and T. H. Carpenter, 1982: Variations in tropical sea surface temperature and surface wind fields associated with the Southern Oscillation/El Niño. *Mon. Wea. Rev.,* **110,** 354–384.

——, X. Wang, and C. F. Ropelewski, 1990: The biennial component of ENSO variability. *J. Mar. Syst.,* **1,** 71–96.

Rutherford, S., and S. D'Hondt, 2000: Early onset and tropical forcing of 100,000-year Pleistocene glacial cycles. *Nature,* **408,** 72–75.

Shiskin, J., 1978: Seasonal adjustment of sensitive indicators. *Seasonal Analysis of Economic Time Series,* A. Zellner, Ed., U.S. Department of Commerce, Bureau of the Census, 97–103.

——, A. H. Young, and J. C. Musgrave, 1967: The X-11 variant of Census Method II Seasonal Adjustment Programme. Tech. Paper 15, U.S. Bureau of the Census, 124 pp.

Sutradhar, B. C., and E. B. Dagum, 1998: Bartlett-type modified test for moving seasonality with applications. *Statistician,* **47,** 191–206.

Thompson, R., 1995: Complex demodulation and the estimation of the changing continentality of Europe's climate. *Int. J. Climatol.,* **15,** 175–185.

——, 1999: A time-series analysis of the changing seasonality of precipitation in the British Isles and neighbouring areas. *J. Hydrol.,* **224,** 169–183.

Thomson, D. J., 1995: The seasons, global temperature, and precession. *Science,* **268,** 59–68.

Trenberth, K. E., 1997: The definition of El Niño. *Bull. Amer. Meteor. Soc.,* **78,** 2771–2777.

——, and T. J. Hoar, 1996: The 1990–1995 El Niño–Southern Oscillation event: Longest on record. *Geophys. Res. Lett.,* **23,** 57–60.

Tziperman, E., L. Stone, M. Cane, and H. Jarosh, 1994: El Niño chaos: Overlapping of resonances between the seasonal cycle and the Pacific ocean–atmosphere oscillator. *Science,* **264,** 72–74.

van Loon, H., and R. L. Jenne, 1970: On the half-yearly oscillations in the Tropics. *Tellus,* **22,** 391–398.

——, J. W. Kidson, and A. B. Mullian, 1993: Decadal variation of the annual variation in the Australian dataset. *J. Climate,* **6,** 1227–1231.

Vimont, D. J., D. S. Battisti, and A. C. Hirst, 2002: Pacific interannual and interdecadal equatorial variability in a 1000-yr simulation of the CSIRO coupled general circulation model. *J. Climate,* **15,** 160–178.

Wang, B., 1995: Interdecadal changes in El Niño onset in the last four decades. *J. Climate,* **8,** 267–285.

Whitfield, P. H., K. Bodtker, and A. J. Cannon, 2002: Recent variations in temperature and precipitation in Canada, 1976–95. *Int. J. Climatol.,* **22,** 1617–1644.

Yu, X., and M. J. McPhaden, 1999: Seasonal variability in the equatorial Pacific. *J. Phys. Oceanogr.,* **29,** 925–947.